

# Fiber-optic technology: non-invasive monitoring sensor of the human body

JAN NEDOMA<sup>a,\*</sup>, MARCEL FAJKUS<sup>a</sup>, RENE JAROS<sup>b</sup>, RADEK MARTINEK<sup>b</sup>

<sup>a</sup>*Department of Telecommunications, Faculty of Electrical Engineering and Computer Science, VSB - Technical University of Ostrava, 17. listopadu 15/2172, 708 33 Ostrava, Czech Republic*

<sup>b</sup>*Department of Cybernetics and Biomedical Engineering, Faculty of Electrical Engineering and Computer Science, VSB - Technical University of Ostrava, 17. listopadu 15/2172, 708 33 Ostrava, Czech Republic*

---

This paper deals with a non-invasive monitoring sensor based on two Fiber Bragg Gratings encapsulated in interesting body-inert material entitled fiberglass. The proposal sensor integrates three monitoring sensors into one compact sensor which can measure Respiratory Rate (RR), Heart Rate (HR) and Body Temperature (BT) simultaneously. Functionality and accuracy of the sensor were verified by the laboratory tests performing on 8 volunteers (both genders) with their written consent. All tests showed satisfactory accuracy based on the objective Bland-Altman method with a small relative error below 5 %. The innovative benefit is the minimum probe thickness of 1 mm.

(Received December 17, 2018; accepted June 14, 2019)

*Keywords:* Fiber-optic sensor, Bragg grating, Physiological parameters monitoring

---

## 1. Introduction

The nowadays trends in the biomedical instrumentations development clearly show that the immediate future of vital sign monitoring favours the utilization of sophisticated diagnostic tools and devices which integrate more diagnostic parameters into one universal device. This approach allows increasing safety as well as the comfort level of patients. The advantages of optical sensors include their independence from an active power supply and a high immunity to electromagnetic interference (EMI). Thanks to these attributes, optical sensors can be used with other electronic equipment without generating the additional electromagnetic noise. The very small dimensions of optical fibres allow them to be encapsulated inside very thin layers and shapes.

The current state of the research in this field is well presented in articles [1-16], which describes experimental use of fiber-optic technologies for monitoring physiological parameters of human body. In all cases, however, the authors presented sensors that can monitor maximally two vital functions of the human body simultaneously (typically respiratory and heart rate). Our research team has dealt with this issue since 2016 and in following years we created patented fibre-optic sensor that allows monitoring of mechanical vibrations of the human body evoked by life activities such as breathing and cardiac rhythms as well as body temperature, please see [17-18].

This article continues on our previous research, here we described a novel type of biomedical monitoring sensor based on the novel type of encapsulation individual FBGs. For encapsulation, we used interesting body-inert material entitled fiberglass (fiberglass is a composite material made up of glass fiber – fabric - and cured synthetic resin). Six layers of fiberglass were used to create the prototype of the sensor (more detail in Figure 2). This type of encapsulation

allowed us to a novel sensor with minimal dimensions (a width of the sensor is only 1 mm) and low weight (4 g). Here we describe the original results and accuracy of the heart rate, respiratory rate and body temperature measurements performed by the tested our novel sensor in comparison to corresponding reference measurements that are commonly used in clinical practice (this is described in more detail in Section 3 below). According to the Bland-Altman analysis the relative error in the case of RR is 4.03 % and in the case of HR by 4.45 %. In the case of temperature measurements, the relative error is 0.18 %.

Desirable characteristic features of optical sensors include their independence from an active power supply and a high immunity to electromagnetic interference (EMI). Thanks to these attributes, optical sensors can be used with other electronic equipment without generating electric noise that may compromise the quality of vital sign monitoring and potentially lead into patient safety concerns. The very small dimensions of optical fibres allow them to be encapsulated inside very thin layers and shapes.

Some research articles which used two FBGs have presented the results of measurements of respiration rate and heart rate both simultaneously [19-22]. In this design, it is essential to pay special attention to the tension of the optical fibre so that adequate sensitivity is achieved. The detailed design of this FBG-based sensor for monitoring respiratory and heart rates in human subjects is presented in [19]. In this work, the sensor consists of one FBG embedded inside a single-mode optical fibre that operates with the wavelength of approximately 1550 nm with a maximum relative measurement error of 12 %. The experimental satisfactory results reported in article [20] describe an FBG-based sensor prototype designed for monitoring the respiratory and heart rate simultaneously. In this work, the sensor (with one FBG) is encapsulated inside a polydimethylsiloxane (PDMS) enclosure. The sensor

assembly is mounted on an elastic contact strap that encircles the patient's chest. The tension in the chest caused by breathing leads to a spectral shift of the reflected light from the FBG. In [21], Dziuda et al. present results obtained from monitoring the respiration and heart rates of a patient in a Magnetic Resonance Imaging (MRI) environment using a fibre-optic FBG-based sensor. This sensor was proposed by its developers to specifically acquire BallistoCardioGraphic (BCG) signals from a patient positioned inside a dynamic magnetic field. Interestingly, article [22]. This paper reports satisfactory results by a novel optical BCG technique within one sensor with one FBG, which is non-invasive, for the simultaneous measurement of heart and respiratory activities. The results obtained from the sensor positioned around the pulmonic area on the chest have been evaluated against an electronic stethoscope which detects and records sound pulses originated from the cardiac activity.

Our monitoring sensor which using only one supply lead presents an alternative to conventional sensors used and can improve the comfort of patients in clinics and hospitals which are focused on monitoring long-term ill patients. The sensor is a part of the clamping elastic belt. This belt can also be used in MR environments. The benefits include also the possibility of remote evaluation of the measured data. The distance is limited by the type of used optical fiber located between the sensor and the evaluation unit (fiber attenuation coefficient) and, further, by the power and wavelength of the radiation source used. Another innovative benefit of this sensor and article is the minimum probe thickness of 1 mm.

## 2. Methods

FBGs are currently one of the most used single point fibre-optic sensors due to their appropriate properties such as: small size with high tensile strength, resistance to electromagnetic interference, and minimal ageing effect with regard to the components from which they are assembled. FBGs function by means of the periodical change of the refractive index in their optical core, selectively filtering certain wavelengths that are reflected back, while allowing the remaining part of the spectrum to pass through. All the reflected light signals combine coherently to form one large reflection at a particular wavelength when the grating period is approximately 1/2 of the input light's wavelength, what is referred to as the Bragg condition, and the wavelength at which this reflection occurs is called the Bragg Wavelength. A fiber Bragg grating structure is depicted in Figure 1. Because FBGs are sensitive to strain and temperature changes, they are suitable for many biomedical measurements. Single-point FBG sensors can be connected together in cascade, thereby producing a multi-point sensor within one optical fibre. The easiest method for enhancing the resolution of individual sensors, is to use wavelength-division multiplexing. We can integrate many of the sensors within the wavelength-division multiplex, whose capacity is given

especially by the type of a measured value and the size of measuring ranges [23].

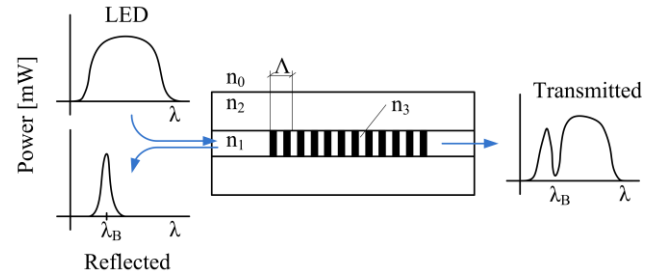


Fig. 1. FBG structure and working principle

The central fiber Bragg wavelength is defined as:

$$\lambda_B = 2n_{eff}\Lambda \quad (1)$$

where  $n_{eff}$  is the effective refractive index of the used optical fiber with Bragg grating, and  $\Lambda$  is the period of changes in the refractive index of the core of the used optical fiber.

Deformation and temperature dependence are given by the central fiber Bragg wavelength and parameter values (where  $\lambda_B$  is the Bragg wavelength,  $\Delta\lambda_B$  is the shift of the Bragg wavelength,  $\Delta\varepsilon$  is the change of deformation and  $\Delta T$  represents a change in temperature). To determine individual sensitivities, normalized deformation and temperature coefficients are used [23]. The normalized deformation coefficient is given by the following equation:

$$\frac{1}{\lambda_B} \frac{\Delta\lambda_B}{\Delta\varepsilon} = 0.78 \times 10^{-6} \mu\text{strain}^{-1}, \quad (2)$$

The normalized temperature coefficient is expressed by the following relationship:

$$\frac{1}{\lambda_B} \frac{\Delta\lambda_B}{\Delta T} = 6.678 \times 10^{-6} \text{ } ^\circ\text{C}^{-1} \quad (3)$$

In the case of encapsulation of both Bragg gratings into one compact sensor (so both gratings are influenced by temperature and deformation simultaneously) it is necessary to ensure their different sensitivity coefficients. Thanks to this, the deformations (in our case of the body's mechanical movements) and temperature (of the human body) can be sense simultaneously by one compact sensor. So, to analyze the body temperature, we used two FBGs with different temperature and deformation sensitivities. Different sensitivities were within the proposed sensor range given by a specific form and shape of encapsulation, please see Fig. 2.

This article presents a novel method of encapsulation (material, shape, dimensions) of both FBGs and thanks to this encapsulation we can sense Respiratory Rate (RR), Heart Rate (HR) and Body Temperature (BT) simultaneously.

It is discovered that if the sensor is affected by deformation or temperature, the size of both of these

impacts could be determined by using the following relationship [24]:

$$\begin{aligned} \frac{(\Delta T)}{(\Delta \varepsilon)} &= \frac{1}{K_{1T}K_{2\varepsilon} + K_{2T}K_{1\varepsilon}} \times \\ &\times \begin{pmatrix} K_{2\varepsilon} & -K_{1\varepsilon} \\ -K_{2T} & K_{1T} \end{pmatrix} \begin{pmatrix} \Delta\lambda_{B1} \\ \Delta\lambda_{B2} \end{pmatrix}, \end{aligned} \quad (4)$$

where  $\Delta\varepsilon$  is deformation,  $\Delta T$  is the temperature change,  $K_{n\varepsilon}$  is the deformation coefficient, and  $K_{nT}$  is the temperature coefficient belonging to the first or second FBG.  $\Delta\lambda_{B1}$  and  $\Delta\lambda_{B2}$  represent the shift of the Bragg wavelength for the first  $FBG_1$  and the second  $FBG_2$ , respectively.

For encapsulation, we used a Bragg grating with a wavelength of 1551.228 nm. Due to the encapsulation process, the Bragg wavelength reduced to the value of 1551.17 nm. The temperature sensitivity increases from 10.35 pm/°C to 11.35 pm/°C due to encapsulation in the fiberglass. We can state that the encapsulation process has no significant effect on the shape of the reflection spectrum and also has no effect on the functionality of FBG.

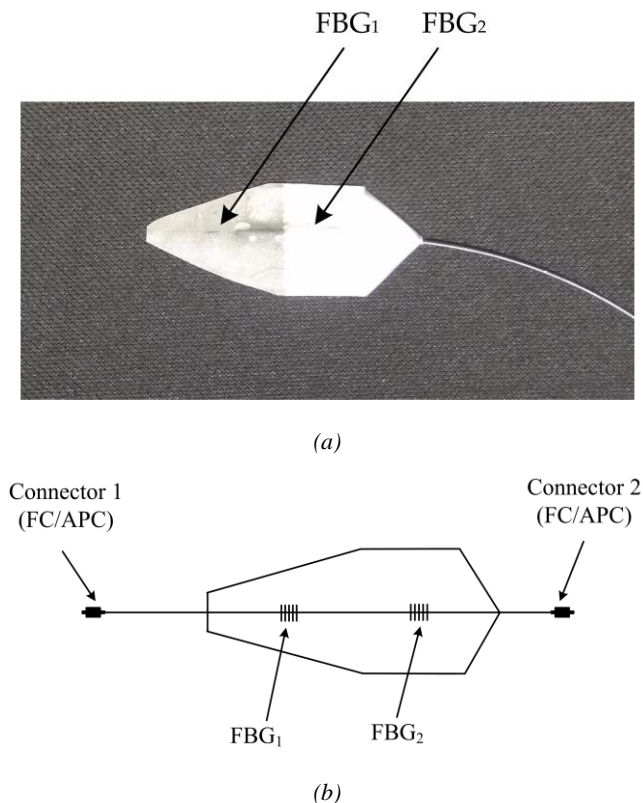


Fig. 2. (a) A photo of the sensor prototype; (b) Schematic diagram of the sensor

The described FBG sensor sensing the mechanical action of the heart, the so-called Ballistocardiography (BCG) signal. From a medical point of view, this is an increasingly used non-invasive method of sensing body movements that are caused by the acceleration of blood spreading inside large blood vessels. The flowing blood

hits the so-called aortic arch that causes the body to move upwards and the subsequent movement of the body down upon the descent of blood. Fig. 3 shows the comparison of ECG and BCG signals. ECG signal contains three dominated components. Dominant R wave, which is the largest wave in the QRS complex, the P wave which represents the depolarization of the atria and the T wave which represents the repolarization of the ventricles. H wave is a concave wave beginning near the beginning of the R wave, I wave is a small wave following the H wave, J wave is the largest wave of a concave shape following immediately after the I wave, and K wave is a convex wave following the J wave [25].

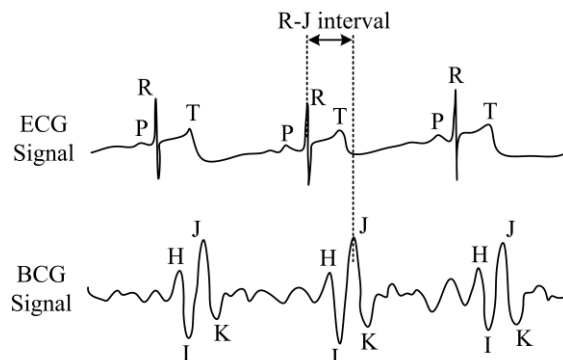


Fig. 3. Sample recordings of electrocardiogram (ECG) and Ballistocardiography (BCG) signals

### 3. Experimental setup and results

The experimental measurements were provided with the written informed consents of 8 volunteer subjects of both sexes (4 men: M<sub>1</sub>-M<sub>4</sub>, and 4 women: F<sub>1</sub>-F<sub>4</sub>) in a research laboratory with the temperature of 22 °C. The subjects were between 23 and 58 years of age, their height was between 156 to 203 cm and their weight was between 43 to 127 kilograms. During the measurements, no significant differences in obtained data were found based on the subject's age, height, or weight. The sensor was placed on the chest (around the heart area) and fixed by a contact elastic strap to the human body. The subjects were tested in the supine position in a relaxed state because we assume the use of the sensor for patients with minimal body movements (long-term ill patients). The experimental part is based on the evaluation of the short-time sequences (summary: 2 hours and 44 minutes of measured data). Measurement scheme is shown in Fig. 4.

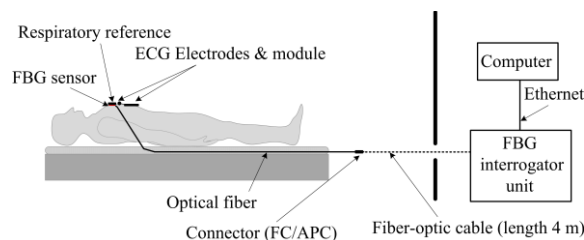


Fig. 4. Measurement scheme

In our study, a conventional 3-lead electrocardiography (ECG) device (NI ELVIS, II Series, National Instruments, Austin, TX, USA) was used as a reference for monitoring the heart rate. For monitoring the respiratory rate, we used the piezo-electric respiratory transducer [26] (thoracic placement). The body temperature was obtained by a digital thermometer with records (Greisinger, Prague, Czech Republic). Signals were processed according to information of the product sheets.

As an optical interrogator unit, we used a spectral conventional instrument called FBGuard (<http://www.safibra.cz/>). FBGuard is an FBG interrogation unit designed for measurement and data processing of values measured from FBG sensors. This unit is working in the wavelength range of 1550 nm, output power of 1 mW, and with maximum scan 11 kHz in single channel version. For our experimental tests, we used a sampling rate of 500 Hz, respiratory and heart rates were processed based on our previous research [17], [20].

Acquired data were compared by the objective Bland-Altman method [27]. The Bland-Altman analysis is a numerical and graphical method to compare two measurements techniques (reference and sensor). In this method, the differences between the two techniques are plotted against the averages of the two techniques. The reproducibility is considered to be good if 95 % of the results lie within a  $\pm 1.96$  SD (Standard Deviation) range. Below are graphical examples of measured data (test volunteer  $M_1$ ). Table 1 and Table 2 contain the statistical data obtained from all 8 test volunteers. Fig. 5 shows an example of a 30-second period window, which representing the breathing activity of test subject  $M_1$  against the conventional piezoelectric respiratory transducer.

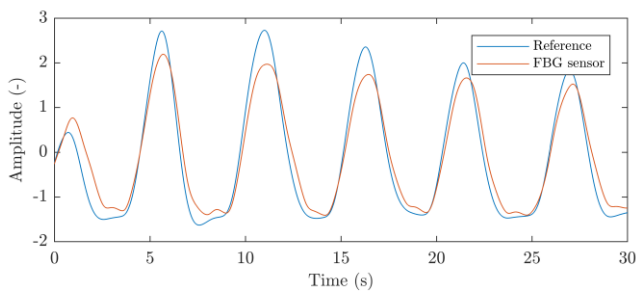


Fig. 5. An example of a 30-second period window representing the breathing activity of test subject  $M_1$

Fig. 6 shows an example of a 20-second period window, which representing the heart activity of test subject  $M_1$  against the conventional 3-lead electrocardiography (ECG) device. The individual maxima detected in the case of the ECG signal represent the R wave, in the case of the signal obtained from our sensor, the individual maxima detected characterize the J wave (the J wave is a characteristic of the R wave of the ECG signal), please see Fig. 3.

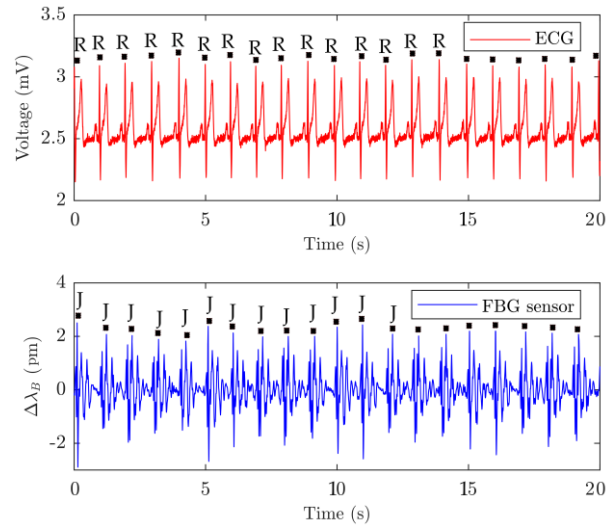


Fig. 6. An example of a 20-second period window representing the heart activity of test subject  $M_1$

Fig. 7 shows an example of a 120-second record of temperature measurement (test subject  $M_1$ ) against the conventional digital thermometer with records.

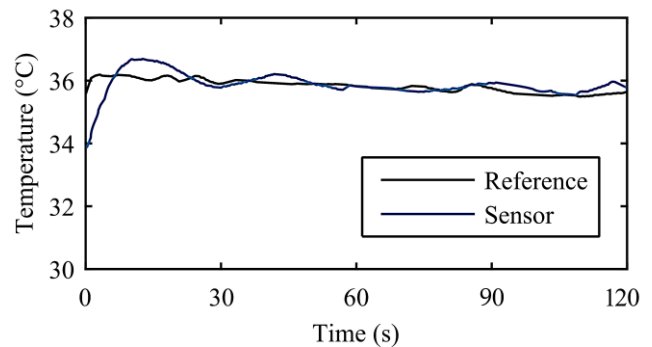


Fig. 7. An example of a 120-second period window representing record of temperature (test subject  $M_1$ )

The key experimental results for the heart and respiratory rate measurements are summarized in Table 1 respectively Table 2. The "recording time" of individual test volunteers is represented in seconds, a "number of sample sensor" means the number of detected maxims (peaks respectively J waves) and "Samples in  $\pm 1.96$  SD" represents results of Bland-Altman analysis expressed in %. In the case of heart rate measurements for the entire data set, 95.55 % of the values lie within the  $\pm 1.96$  SD range for the HR determination. In the case of respiratory rate measurements for the entire data set, 95.97 % of the values lie within the  $\pm 1.96$  SD range. The results obtained with the Bland-Altman analysis demonstrated the functionality of the FBG sensor.

Table 1. Summary of respiratory rates measurements

Subject	Recording time [s]	Number of sample sensor [-]	Samples in $\pm 1.96$ SD [%]
M <sub>1</sub>	1038	271	96.52
M <sub>2</sub>	1121	279	96.48
M <sub>3</sub>	1422	357	95.87
M <sub>4</sub>	1308	371	96.16
F <sub>1</sub>	1282	303	95.52
F <sub>2</sub>	1408	414	96.28
F <sub>3</sub>	1088	289	95.81
F <sub>4</sub>	1178	329	95.17
<b>Sum</b>	<b>9 408</b>	<b>2 613</b>	<b>95.97</b>

Table 2. Summary of heart rates measurements

Subject	Recording time [s]	Number of sample sensor [-]	Samples in $\pm 1.96$ SD [%]
M <sub>1</sub>	1038	1043	96.48
M <sub>2</sub>	1121	1278	95.54
M <sub>3</sub>	1422	1691	95.34
M <sub>4</sub>	1308	1608	95.81
F <sub>1</sub>	1282	1768	95.23
F <sub>2</sub>	1408	1921	95.87
F <sub>3</sub>	1088	1561	95.31
F <sub>4</sub>	1178	1617	94.87
<b>Sum</b>	<b>9 408</b>	<b>12 487</b>	<b>95.55</b>

The key experimental results of body temperature measurements are summarized in Table 3. This table shows the temperature (temp.) values obtained after a measurement time interval of 120 seconds against reference (ref.). The relative error (Rel. Error) of temperature measurement was 0.18 %.

Table 3. Summary of body temperature measurements

Subject	Source	At time 30 s Temp. [°C]	At time 60 s Temp. [°C]	At time 90 s Temp. [°C]	At time 120 s Temp. [°C]	Rel. Error [%]
M <sub>1</sub>	Ref.	35.9	35.9	35.9	35.8	0.27
	Sensor	35.8	35.8	36.0	35.9	
M <sub>2</sub>	Ref.	36.2	36.3	36.3	36.2	0.20
	Sensor	36.1	36.2	36.3	36.1	
M <sub>3</sub>	Ref.	36.4	36.5	36.5	36.4	0.27
	Sensor	36.3	36.4	36.4	36.3	
M <sub>4</sub>	Ref.	36.4	36.5	36.4	36.6	0.13
	Sensor	36.5	36.5	36.4	36.5	
F <sub>1</sub>	Ref.	36.7	36.7	36.8	36.7	0.13

#### 4. Discussion

The sensor can simply be placed in the clamping elastic belt. This belt can also be used in MR environments unless a respiratory reference is necessary.

Despite the relative error below 5 % (4.03 % in the case of respiratory rate measurements and 4.45 % in the case of heart rate measurements, and 0.18 % in the case of temperature measurements), the sensor is designed primarily for monitoring rather than diagnostics.

The benefits include the possibility of remote evaluation of the quantities measured. The distance is limited by the type of interconnecting optical fiber used located between the sensor and the evaluation unit (fiber attenuation coefficient) and, further, by the power and wavelength of the radiation source used.

This short article presents an alternative method of non-invasive and cost-effective (price of sensor is approximately 200 dollars) patient monitoring which is in its infancy and has not been comprehensively explored. The functionality of the proposed sensor was verified by a series of experimental measurements of basic vital signs and authors are ready to carry out a long-term detailed analysis of proposed sensor in the follow-up research. We are currently awaiting the permission of the ethics committee to carry out extensive clinical trials.

Another article will more focus and widely explore the way how to reduce the motion artifacts (hardware and sensor improving). Nowadays, we can partially filter out these artifacts by the software compensation. Results of this article represent a data where test subjects were in the relaxed supine position.

Subject	Source	At time 30 s Temp. [°C]	At time 60 s Temp. [°C]	At time 90 s Temp. [°C]	At time 120 s Temp. [°C]	Rel. Error [%]
	Sensor	36.6	36.7	36.7	36.7	
F <sub>2</sub>	Ref.	36.5	36.5	36.4	36.5	0.20
	Sensor	36.4	36.5	36.5	36.4	
F <sub>3</sub>	Ref.	36.3	36.3	36.3	36.3	0.07
	Sensor	36.2	36.3	36.3	36.3	
F <sub>4</sub>	Ref.	36.8	36.8	36.8	36.8	0.20
	Sensor	36.7	36.8	36.7	36.7	

## 5. Conclusion

The aim of this short article was to bring a description of our novel non-invasive fiber-optic sensor which can be used for the monitoring of the basic vital signs of the human body. Proposed monitoring sensor allows collecting the data about Respiratory Rate, Heart Rate and Body Temperature simultaneously. The functionality and reliability of the sensor were tested on 8 volunteers with their written consent. The original results of Bland-Altman statistical analysis for the respiratory rate (95.97 %) and heart rate (95.55 %) measurements showed the satisfactory accuracy of the sensor. Despite the relative error below 5 % (4.03 % in the case of respiratory rate measurements, 4.45 % in the case of heart rate measurements, and 0.18 % in the case of body temperature measurements), the sensor is designed primarily for monitoring rather than diagnostics. The innovative benefit is also the minimum probe thickness of 1 mm.

## Acknowledgments

This article was supported by the Ministry of Education of the Czech Republic (Projects No. SP2019/80, SP2019/85). This work was supported by the European Regional Development Fund in Research Platform focused on Industry 4.0 and Robotics in Ostrava project, CZ.02.1.01/0.0/0.0/17\_049/0008425 within the Operational Programme Research, Development and Education.

## References

- [1] P. Roriz, L. Carvalho, O. Frazao, J. L. Santos, J. A. Simoes, *Journal of Biomechanics* **47**(6), 1251 (2014).
- [2] L. Dziuba, *Journal of Biomedical Optics* **20**(1), 010901 (2015).
- [3] K. Chethana, A. S. Guru Prasad, S. N. Omkar, S. Asokan, *Journal of Biophotonics* **10**(2), 278 (2017).
- [4] F. C. Favero, V. Pruneri, J. Villatoro, *Journal of Biomedical Optics* **17**(3), 037006 (2012).
- [5] S. Sprager, D. Donlagic, D. Zazula, In *Signal Processing (ICSP)*, 2010 IEEE 10th International Conference on (pp. 1-4). IEEE (2010).
- [6] S. Sprager, D. Donlagic, D. Zazula, In *Proceedings of the IASTED International Conference on Signal and Image Processing*, Dallas, TX, USA (pp. 14-16) (2011).
- [7] S. Sprager, D. Zazula, *Computer Methods and Programs in Biomedicine* **111**(1), 41 (2013).
- [8] C. Will, K. Shi, F. Lurz, R. Weigel, A. Koelpin, In *IEEE International Symposium on Intelligent Signal Processing and Communication Systems (ISPACS)*, 483 (2015).
- [9] J. Nedoma, M. Fajkus, R. Martinek, H. Nazeran, *Sensors* **19**(1), 470 (2019).
- [10] J. Nedoma, S. Kepak, M. Fajkus, J. Cubik, P. Siska, R. Martinek, P. Krupa, *Sensors* **18**(11), 3713 (2018).
- [11] Y. H. Hsieh, N. K. Chen, In *Advanced Infocomm Technology (ICAIT)*, 2013 6th International Conference on (pp. 113-115). IEEE (2013).
- [12] A. Grillet, D. Kinet, J. Witt, M. Schukar, K. Krebber, F. Pirotte, A. Depre, *IEEE Sensors Journal* **8**(7), 1215 (2008).
- [13] F. Taffoni, D. Formica, P. Saccomandi, G. Pino, E. Schena, *Sensors* **13**(10), 14105 (2013).
- [14] A. Grillet, D. Kinet, J. Witt, M. Schukar, K. Krebber, F. Pirotte, A. Depre, In *Third European Workshop on Optical Fibre Sensors (Vol. 6619, p. 66191R)*. International Society For Optics And Photonics (2007).
- [15] K. M. Moerman, A. M. Sprengers, A. J. Nederveen, C. K. Simms, *Medical Engineering and Physics* **35**(4), 486 (2013).
- [16] U. X. Tan, B. Yang, R. Gullapalli, J. P. Desai, *IEEE Transactions on Robotics* **27**(1), 65 (2013).
- [17] M. Fajkus, J. Nedoma, R. Martinek, V. Vasinek, H. Nazeran, P. Siska, *Sensors* **17**(1), 111 (2017).
- [18] V. Vasinek, J. Nedoma, M. Fajkus, R. Martinek, RCZ Patent No. 306857.
- [19] L. Dziuda, F. W. Skibniewski, M. Krej, J. Lewandowski, *IEEE Transactions on Biomedical Engineering* **59**(7), 1934 (2012).
- [20] J. Nedoma, M. Fajkus, P. Siska, R. Martinek, V. Vasinek, *Advances in Electrical and Electronic Engineering* **15**(1), 93 (2017).
- [21] L. Dziuda, M. Krej, F. W. Skibniewski, *IEEE Sens. J.* **13**(12), 4986 (2013).
- [22] K. Chethana, A. S. Guru Prasad, S. N. Omkar, S. Asokan, *Journal of Biophotonics* **10**(2), 278 (2017).

- [23] A. D. Kersey, M. A. Davis, H. J. Patrick, M. Leblanc, K. P. Koo, C. G. Askins, M. A. Putnam, E. J. Friebele, *Journal of Lightwave Technology* **15**(8), 1442 (1997).
- [24] M. R. Mokhtar, T. Sun, K. T. V. Grattan, *IEEE Sensors Journal* **12**(1), 139 (2012).
- [25] E. Pinheiro, O. Postolache, P. Girao, *The open Biomedical Engineering Journal* **4**, 201 (2010).
- [26] C. Rotariu, C. Cristea, D. Arotaritei, R. G. Bozomitu, A. Pasarica, In *IEEE 22nd International Symposium for design and technology in electronic packaging (SIITME)*, 106 (2016).
- [27] J. M. Bland, D. G. Altman, *Statistical Methods in Medical Research* **8**(2), 135 (1999).

---

\*Corresponding author: jan.nedoma@vsb.cz